

Morphological and histometric features of the caudal kidney in piranha *Pygocentrus nattereri* (Characiformes: Serrasalminidae)



Correspondence:
Carlos E. Fernandes
carlos.fernandes@ufms.br

Sandriely F. Marcondes¹, Mayara S. Siqueira¹, Taynara R. F. Leão¹,
 Robson A. Rodrigues², Karine N. N. Farias¹, André L. N. Silva¹,
 Lilian Franco-Belussi¹ and Carlos E. Fernandes¹

Pygocentrus nattereri is a widely distributed species in the Neotropical region and a potential bio-indicator. Kidneys have functions in fish physiology, allowing them to live in different environments. We aimed to compare the histological characteristics of caudal kidneys between males and females, associating them with the renosomatic index (RSI). For this purpose, 15 males and 14 females were used for biometric and histological analyses. Structural volumetric density (SVD), renal corpuscle histometric measures, and hemosiderin and lipofuscin deposit frequency in macrophages melanogenic (MMs) were assessed. No biometric differences were observed between the sexes, but body weight and standard length were correlated with RSI. The SVD showed difference in hematopoietic tissue between female and males, whereas the density of the other structures was not different. The RSI was positively associated with hematopoietic tissue and proximal tubule density in contrast to distal tubules, blood vessels, collecting ducts and MMs. Females exhibited a higher renal corpuscle area, glomerulus area, distal tubule diameter, collecting tubule area, and collecting tubule lumen area. These differences may be due to metabolic differences between males and females. Sex effect in *P. nattereri* may define punctual differences in future studies on the metabolism and immunity of this species.

Keywords: Fish, Histology, Histometry, Renosomatic index.

Submitted November 26, 2022

Accepted May 31, 2023

by Bernardo Baldisserotto

Epub July 17, 2023



Online version ISSN 1982-0224

Print version ISSN 1679-6225

Neotrop. Ichthyol.
vol. 21, no. 2, Maringá 2023

¹ Laboratório de Patologia Experimental (LAPEx), Instituto de Biociências, Universidade Federal de Mato Grosso do Sul, Av. Costa e Silva, s/n, Universitário, 79002-970 Campo Grande, MS, Brazil. (SFM) sandy.marcondes@outlook.com, (MSS) mayara_schueroff@hotmail.com, (TRFL) trfleao@gmail.com, (KNNF) kanathiele@gmail.com, (ALNS) andrenascimento31@gmail.com, (LFB) lilian.belussi@gmail.com, (CEF) carlos.fernandes@ufms.br (corresponding author).

² Departamento de Aquicultura do Centro de Ciências Agrárias, Universidade Federal de Santa Catarina, Rodovia Francisco Thomaz dos Santos, Armação do Pântano do Sul, 88066-260 Florianópolis, SC, Brazil. (RAR) robson.andrade.rodrigues17@hotmail.com.

Pygocentrus nattereri é uma espécie amplamente distribuída na região Neotropical e pode ser considerada como um potencial bioindicador ambiental. Os rins têm funções cruciais na fisiologia dos peixes, permitindo-lhes viver em diferentes ambientes. Nosso objetivo foi comparar as características histológicas dos rins excretoras entre machos e fêmeas, associando-as ao índice renossomático (IRS). Para tanto, 15 machos e 14 fêmeas foram utilizados para análises biométricas e histológicas. Amostras do tecido renal foram processadas para densidade estrutural volumétrica, medidas histométricas do corpúsculo renal e frequência dos depósitos de hemossiderina e lipofuscina nos macrófagos melonogênicos (MMs). Não foram observadas diferenças biométricas entre os sexos, mas a massa corporal e o comprimento padrão foram correlacionados com IRS. Apenas a densidade estrutural volumétrica do tecido hematopoiético foi diferente entre machos e fêmeas. Não houve diferença nas demais estruturas. O IRS associou-se positivamente com o tecido hematopoiético e densidade dos túbulos proximais e negativamente com os túbulos distais, vasos sanguíneos, ductos coletores e MMs. As fêmeas apresentaram maior área do corpúsculo renal, área do glomérulo, diâmetro do túbulo distal, área do túbulo coletor e área do lúmen do túbulo coletor. Essas diferenças podem ser devida às diferenças metabólicas entre machos e fêmeas. Particularidade do efeito de sexo em *P. nattereri* pode definir diferenças pontuais em futuros estudos sobre o metabolismo e imunidade nesta espécie.

Palavras-chave: Índice renossomático, Histologia, Histometria, Peixe.

INTRODUCTION

Pygocentrus nattereri Kner, 1858 (Serrasalminae) present a wide distribution in the Neotropical region, particularly in the Amazon and Pantanal biomes (Ferreira *et al.*, 2014). These are usually named piranha, true piranha, and red-bellied piranha and are distributed in different environmental aquatic habitats with a predominantly piscivorous feeding habit (Frose, Pauly, 2020). From an ecological perspective, they occupy a clear trophic position and are considered useful bioindicators in lotic and lentic environments (Burger, 2006; Ferreira *et al.*, 2017).

The kidney plays an important role in maintaining osmoregulation, immune, and hematopoietic functions in fish (Hentschel *et al.*, 2000). Although their physiology is similar, the main structure and organization of renal tissue have been reported in freshwater fish, possibly due to evolutionary processes in the living environment (Vize, 2004; McDonald *et al.*, 2006). The teleost kidney is divided into cephalic or anterior, and caudal or truncal (Takashima, Hibiya, 1995). The kidneys may be fused in some species and their differentiation can only be achieved by microscopy (Roberts, Ellis, 2012; Fernandes *et al.*, 2019). Cephalic and caudal portions are separated into some adult specimens. However, the caudal kidney is a mixed organ composed of a reticuloendothelial network, endocrine, and exocrine elements jointly with erythroid, lymphoid, and myeloid cells (Roberts, Ellis, 2012).

Although the anatomy, histology, and cytology related to the kidney have been well reported in many freshwater fishes (Takashima, Hibiya, 1995), histological data of *P. nattereri* have not been previously reported. Furthermore, the effects of sex are not investigated thoroughly. In some biomes, such as the Brazilian Pantanal, environmentally heterogeneous wetlands play a primary role in ichthyological biodiversity and biotic homeostatic processes (Alho, 2005; Novakowski *et al.*, 2008; Siqueira *et al.*, 2021). Thus, males and females can differentiate certain structural particularities in target organs, affecting their biological rhythms. There is evidence that sex differences in wild environments in terms of demographic, ecological, and physiological features (Campbell *et al.*, 2021). For instance, in *Salmo trutta* Linnaeus, 1758, differences in the relative volumes of some renal components were detected between the sexes. During the reproductive season, females have a higher volume of renal corpuscles and collecting tubules, suggesting that endocrine differences may modulate renal physiology (Resende *et al.*, 2010).

Organosomatic indices are widely used in ecological and experimental studies. However, the renosomatic index has been poorly reported in association with histological biomarkers compared to other indices (Nimet *et al.*, 2018). Variations in this index suggest metabolic changes in response to a range of pathophysiological or environmental contamination effects on the kidneys (Fernandes *et al.*, 2019; Idrus *et al.*, 2022). Nevertheless, the relationship between this index and the quantitative morphological traits in fish remains unknown. Linear and dimensional morphometric measurements allow the detection of minimal differences in cells and tissues, favoring qualitative analysis responding to organ functionality (Nyengaard, 1999; Rašković *et al.*, 2019). The association between renal histomorphometry attributes and this index would permit the assessment of adaptive responses to biotic factors. Therefore, we aimed to evaluate some quantitative histological features of the caudal kidney between males and females, associating them with the renosomatic index. Thus, we intend to describe characteristics of the caudal kidney related to gender. Our hypothesis is that females and males present differences between the components of the caudal kidney due to metabolism. These differences should be more evident during the reproductive period.

MATERIAL AND METHODS

Study area, sampling, and biometry. *Pygocentrus nattereri*, 15 males and 14 females (voucher ZUFMS-PIS 5267) were captured using a hook and line in the Miranda River, Passo do Lontra region, 19°34'37"S 57°00'42"W, Corumbá Municipality, Mato Grosso do Sul State, Brazil. Males weighed 302.3±106.6g, and measured 17.2±2.6cm in standard length; female weighed 281.4±190.2g and measured 17.6 ±3.2cm in standard length. The experimental period consisted of wet seasons (October 2018 to February 2019) and fishes were collected daytime, according to annual environmental variations in the temperature and rainfall (Alho, 2005). After capture, the specimens were kept in a tank (1,000 L) without food, with running water at a temperature of 23–28 °C and under artificial aeration (4.8 ± 2.0 mg/L oxygen density) for 12–15 h. Throughout the experimental period, river water features remained between 16.2–28.6 °C for temperature, 4.8–7.8 mg/L for oxygen density, 6.0–8.4 for pH, 469.0–594.0 µs/cm for conductivity and 275.0–350.0 mg/L for oxidation reduction potential. For the

biometric procedures, fish were euthanized with a eugenol solution (450 mg/L, 1:10 absolute alcohol solution) and their weight (g) and standard length (cm) were recorded. The fish were necropsied and the exocrine kidneys were dissected and weighed (g) to estimate the renosomatic index ($RSI\% = \text{kidney weight/body weight} \times 100$).

Histological preparation. Caudal kidney was the exocrine kidney was transversely sectioned into three parts: anterior, medium and posterior fragments. We evaluate fish kidneys of three females and three males per month fixed in 10% buffered formalin solution for 24 h and transferred to 70% alcohol solution until they were histologically processed for paraffin inclusion. Longitudinal and transversal sections were prepared for histological analysis (3 μm) and stained with hematoxylin and eosin (HE) for general description. Periodic acid-Schiff (PAS) and Masson's trichrome (TM) were used for descriptive analysis, according to Carson, Hladik (2009). The sections were analyzed using bright-field microscopy for morphological descriptions.

Structural volumetric density (SVD). For this analysis, RGB images (3264 x 2448 pixels) were captured using a microscope (Leica DM5500B, 200 x magnification) coupled with a digital camera system (Leica DF495). Nine hematoxylin and eosin (HE)-stained randomized images of three distinct histological sections per fragment were obtained from each specimen. A random offset grid of 285 intersections (quadratic lattice test system) was overlaid for counting points for each specimen. The interpoint distance was 15 μm (Reid, 1980). At each point of intersection, the hematopoietic tissue, renal corpuscles, proximal and distal tubules, collecting ducts, blood vessels (arterial, venous, and capillaries), and melanomacrophage centers (MMCs) were remarkable. The final density for each structure was calculated using the formula $SVD (\%) = ([Ip \times 100]/Tip)$, where Ip is the number of positive intersections for the structure and Tip is the total number of intersections in the image (Rocha *et al.*, 1997). ImageJ version 1.48v was used for the analysis (Ferreira, Rasband, 2014).

Histometric analysis of renal corpuscle. Images (RGB 4096 x 3286 pixels) at 400x magnification were obtained from the sampling reported for VDE analysis. Measures were taken using Motic 2.0 (Motic Asia, Hong Kong). Using the "polygon" tool, the area (μm^2) of the renal corpuscle and glomerulus was estimated. The parietal layer thickness (μm) of the corpuscle renal was estimated by linear measure. Bowman's space area was calculated by subtracting the renal corpuscle area from the glomerulus area.

Quantitative analysis hemosiderin and lipofuscin in melanogenic macrophages. Four histological sections of the same three fragments and blocks used in the SVD analysis per specimen were processed to quantify the labeling of melanogenic macrophages (MMs) for hemosiderin and lipofuscin. The hemosiderin content was detected using Perl's method for ferric iron. Briefly, the sections were incubated in ferrocyanide acid solution, obtained by dissolving 2 g of potassium ferrocyanide in 100 mL of hydrochloric acid solution 0.75 mmol/L for 15 min and immersed in aqueous 1% neutral red followed by aqueous 1% eosin staining. Histological sections of the same samples were prepared to detect lipofuscin content in the MMCs. First, they were incubated for 1 min in Schmorl's solution containing 75 mL of 1% ferric chloride, 10

mL of potassium ferricyanide, and 15 mL of distilled water. Afterward, the sections were immersed in an aqueous 1% neutral red solution, followed by 1% eosin (Franco-Belussi *et al.*, 2013).

The labeling MMs for both pigments were estimated from the RGB images (4096 × 3286 pixels) obtained at 400× magnification, according to the system previously reported for each histological section. Images were analyzed using Image-Pro Plus 6.0 (Media Cybernetics, Inc, USA) software. First, the measurement tool estimated the total standardized image area (58969.79 μm²) in planimetry. Subsequently, the “count/size” tool was selected for the measurements. Afterward, we apply the “dropper” tool to select the color to be measured in the image. Here, the tool’s sensitivity 3 was used to be able to select the entire area (μm²) for each pigment. The final count (Fc) per section was estimated using the following formula: Fc % = (pigment area / 58969.79) × 100.

Statistical analysis. Data normality and homogeneity were confirmed using Kolmogorov-Smirnov’s and Levene’s tests. Data of the structural volumetric density, hemosiderin, and lipofuscin areas were subjected to angular transformation (arcsine √x/100), and the histometric data were transformed to *log (n)*. After transformation, all the data met the assumptions of normality and homogeneity. The sex effect for biometric and quantitative histochemistry data was estimated using a generalized linear model (ANOVA) with contrasts estimated using Sidak’s test. For the structural volumetric density and renal corpuscles histometric data, a covariance analysis model (ANCOVA) including the renosomatic index as a covariable was prepared. Pearson’s bivariate test was used to determine the linear correlations between the renosomatic index with biometric variables and structural volumetric density data.

RESULTS

Biometry parameters. The biometric parameters and renosomatic index (RSI) of the specimens are listed in Tab. 1. The RSI was used to analyze correlations with stereological and biometric data. Biometric data presented no significant difference ($P > 0.05$) between males and females. However, regardless of the sex of the individual, body weight ($r = -0.45$; $P < 0.01$) and standard length ($r = -0.46$; $P < 0.01$) were correlated with the IRS.

TABLE 1 | Mean, standard deviation (±) and confidence interval (IC 95%) of biometric variables by sex, P value (P) showing no differences between males and females, and Pearson’s correlation coefficient (r) with renosomatic index in the caudal kidney in *Pygocentrus nattereri* showing negative correlation with body weight and standard length (*). N = specimens number, * $p < 0.05$, ** $P < 0.01$, ns = non significant.

Biometric variables	Male (N = 15)	Female (N = 14)	r
Body weight (g)	302.3 ±106.6 (168.2–329.9)	281.4 ±190.2 (197.9–365.4)	-0.45*
Standard length (cm)	17.2 ±2.65 (15.6–18.7)	17.6 ±3.24 (15.9–19.2)	-0.46**
Kidney weight (g)	1.09 ±0.54 (0.80–1.39)	1.16 ±0.57 (0.85–1.46)	ns
Renosomatic index (%)	0.44 ±0.09 (0.38–0.50)	0.46 ±0.14 (0.39–0.52)	-

Morphological kidney features. The caudal kidney (CK) of *P.nattereri* is anatomically distinct from the cephalic kidney. It is located ventrally to the spine with emphasis on the ureters and cephalic artery, which are readily observed (Fig. 1). The cephalic kidney was located in the cranial region of the coelomic cavity and connected to the caudal kidney through arterial and venous vessels.

The CK components were easily identified using light microscopy (Fig. 2). Arterial vessels that reach the kidney through the renal arteries are transported to the renal corpuscles (Figs. 2B, D, E, F). These were formed by Bowman's capsule and the glomerulus (Fig. 2C). The epithelium attaches to the glomerulus and proximal tubule and is formed by a cuboidal ciliated cell with a basal nucleus (Fig. 2C). Proximal tubules with columnar epithelium and well-developed brush borders were observed. The absence of a brush border characterizes both the distal and collecting tubules.

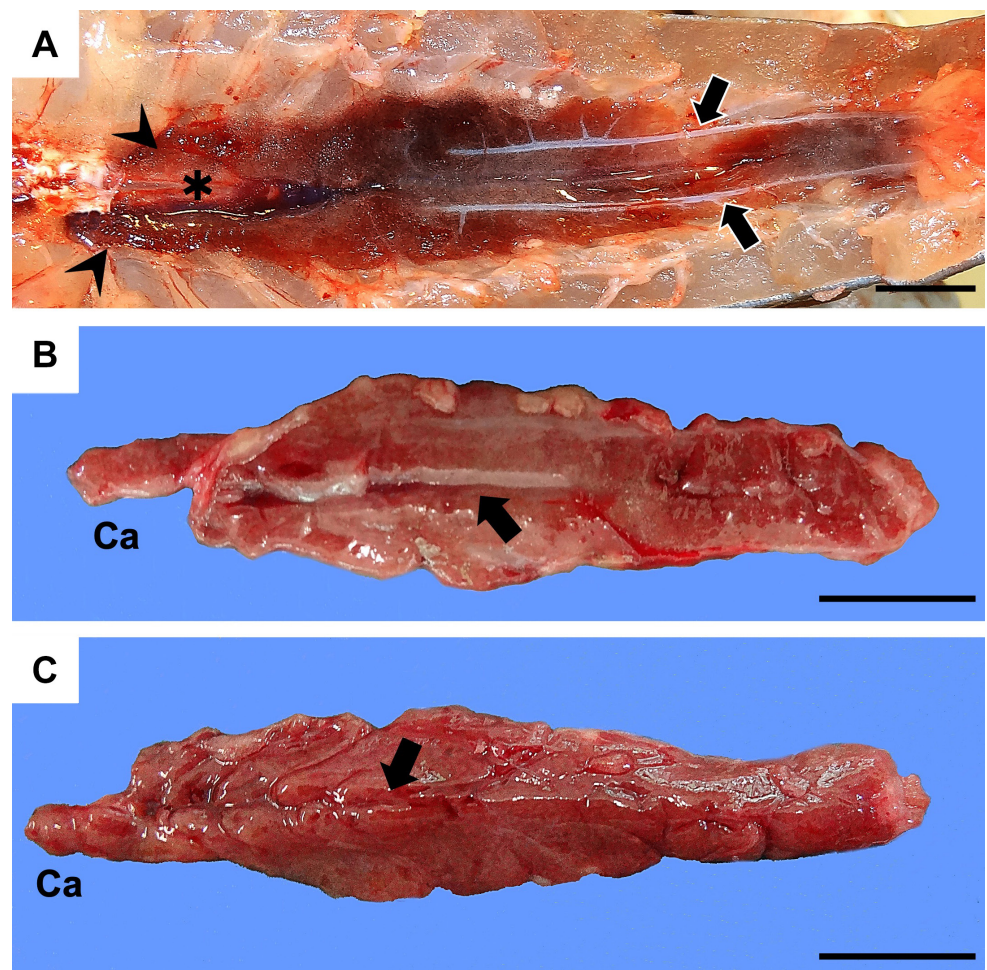


FIGURE 1 | Macroscopic view of the caudal kidney in *Pygocentrus nattereri*. **A.** The typical anatomical position of the organ, ventrally situated on to vertebra column. Two branches (arrowhead) in the cranial portion are divided by the renal arterial (asterisk). The ureters (arrows) emerge from the middle portion of the organ extending to the caudal region. **B.** Ventral view after dissection of the peritoneum membranes; a vertebral vascular groove can be observed (arrow); Ca, caudal portion. **C.** Dorsal view with a prominent vertebral groove (*sulcus arteriae vertebralis*, arrow). Scale bars = 1 cm.

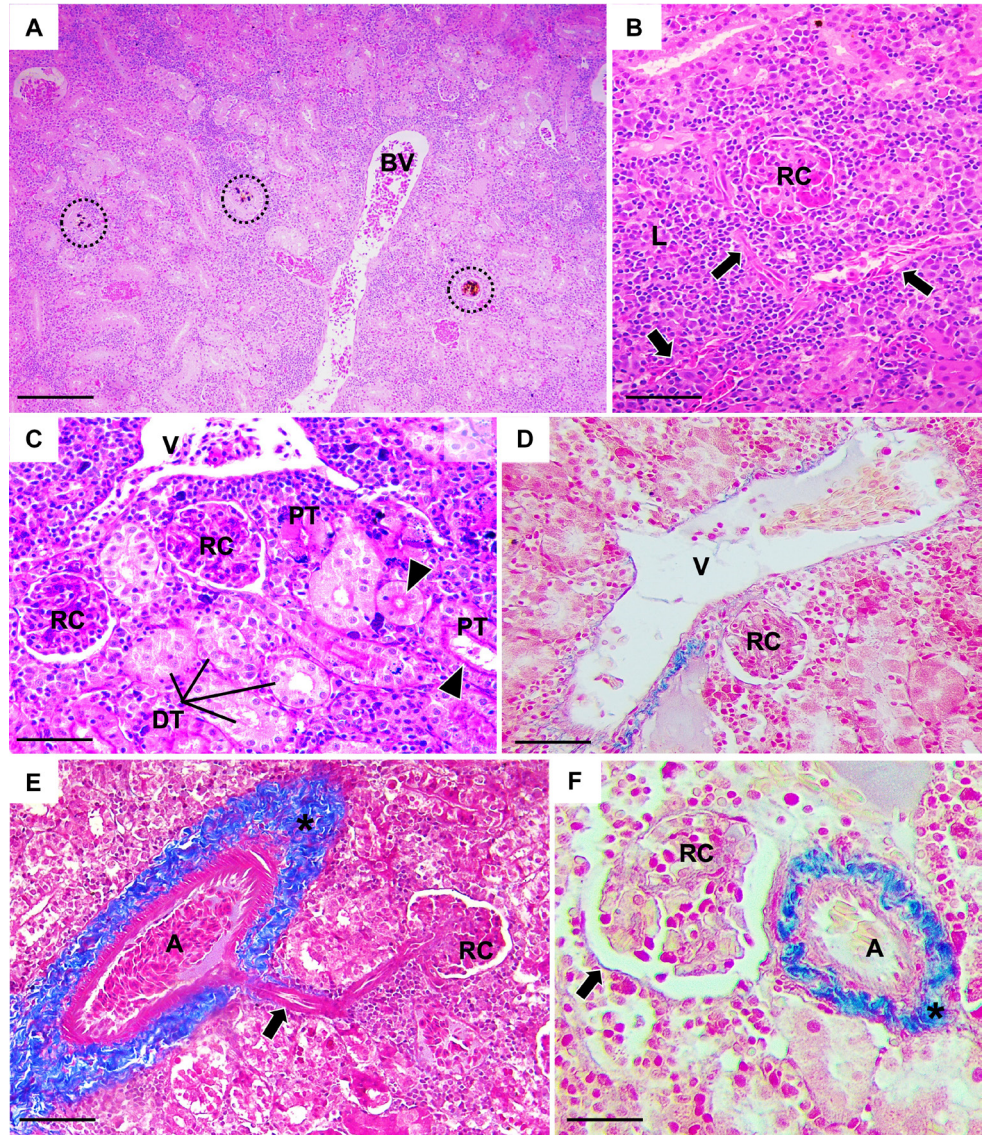


FIGURE 2 | Histological cross-sections of the caudal kidney in *Pygocentrus nattereri* highlighting the vascular features. **A.** Low magnification showing the typical aspect of the kidney parenchyma; segments of blood vessels (BV) are diffusely recognized in all regions; some granulomatous formations are often found (circles in black). HE, scale bar = 200 μ m. **B.** Capillary network from larger vessels spread throughout the parenchyma (arrows) supplying the lymphohematopoietic areas (L); note an immature renal corpuscle (RC) near a capillary branch. HE, scale bar = 50 μ m. **C.** Some RC are usually viewed very closed to larger vessels (V), proximal (PT) and distal tubules (DT); note the brush edge (arrowhead), a characteristic of PT. PAS, scale bar = 50 μ m. **D.** A branch of the renal vein (V) near an RC; a thin collagen bundle can be seen surrounding the vessel. TM, scale bar = 50 μ m. **E.** and **F.** Represents arterial irrigation of the RC, which demonstrate a thick collagenous layer (asterisk); in **E.**, a large arteria (A) with a branch toward the glomerular area (arrow); in **F.**, an arteriole (A) alongside an RC showing a slightly collagenous marking and Bowman's space (arrow); TM, **E.**, scale bar = 50 μ m; **D.**, scale bar = 10 μ m.

Renal corpuscles are diffusely distributed throughout caudal renal tissue, permeating vessels, renal tubules, collecting tubules and ducts, and lymphohematopoietic tissue. The parietal and visceral lamina were PAS-labeled (Fig. 3B). There was no positive labeling for the collagen coating of the glomerular basement membrane (Fig. 3C). A rich lymphohematopoietic tissue showing granulocytes and agranulocytic cells, and immature forms and rodlet cells, is observed (Figs. 3D, E).

Hyaline cytoplasmic deposits were often observed with predominance in the proximal tubules (Fig. 4A). Melano-macrophage aggregates were diffusely distributed into the lymphohematopoietic regions and peripherally to the vessels. In HE staining, the aggregates were dark brown with a rounded shape and variable sizes. Eventually, they were found around the tubules and ducts in the lumen collecting or as infiltrative features (Fig. 4).

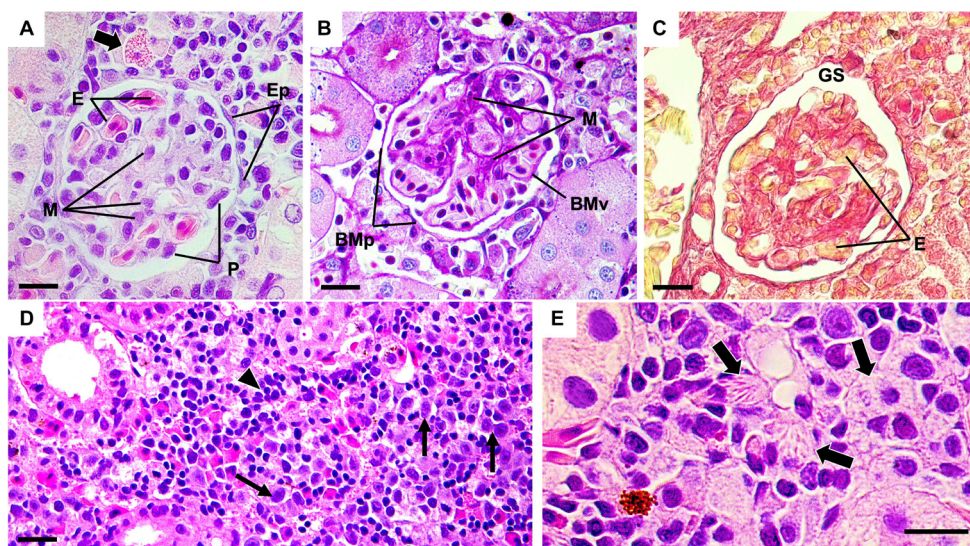


FIGURE 3 | Histological features of renal corpuscles and lymphohematopoietic region of caudal kidney in *Pygocentrus nattereri*. **A.** Renal corpuscle possesses podocytes (P) around of glomerular capillaries; Ep = nuclei of parietal squamous cell layer covering the capsule; erythrocytes (E) are found into the capillaries spread along to mesangial cells (M); note bacteria internalized by a macrophage (arrow); HE, scale bar = 10 μ m. **B.** Mesangial (M), basal membrane visceral (BMv) and parietal (Bmp), positively reacted for PAS reaction; scale bar = 10 μ m; **C.** Renal corpuscle demonstrating negative reaction for collagenous fibers; glomerular space (GS); erythrocyte (E) cytoplasm stained of yellow in MT stain; scale bar = 10 μ m. **D.** A general view of lymphohematopoietic tissue; granulocytes showing a pronounced eosinophilic cytoplasm and tend to form little cellular niches whereas agranulocytes are randomly distributed in cordonal clusters (arrowhead); both cell categories common primordial lineages which displays larger basophilic nuclei (arrows); HE, scale bar = 50; **E.** Rodlet cells are often found thorough lymphohematopoietic tissue (arrows); HE, scale bar = 10 μ m.

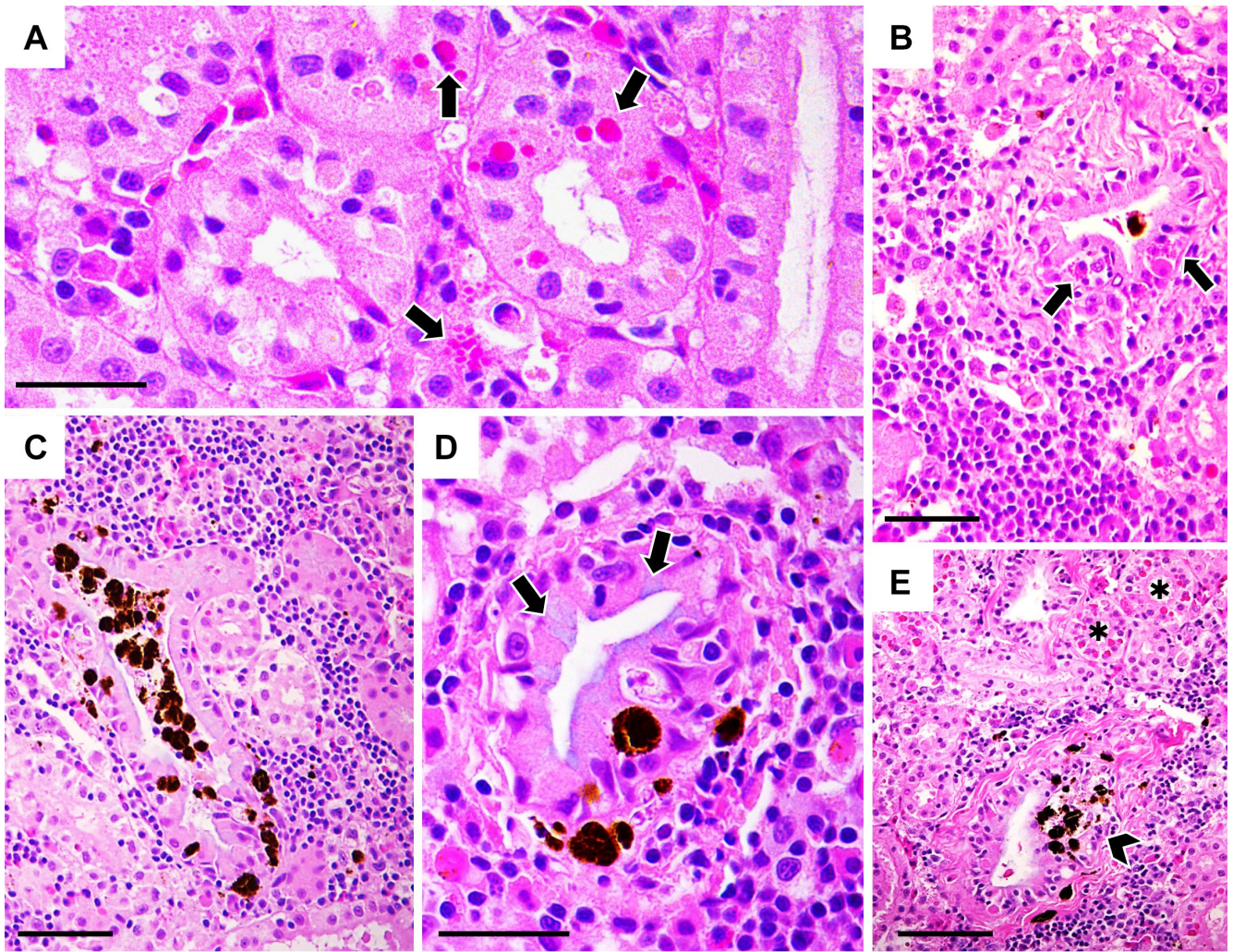


FIGURE 4 | Intracellular and intraluminal deposits in the caudal kidney of *Pygocentrus natterii*. **A.** Cross-section of proximal tubules showing intracytoplasmic single or multi droplets hyaline deposits in epithelial cells (arrows); HE, scale bar = 10 μ m. **B.** Collecting duct presenting a luminal melanogenic macrophage; leukocyte cells often infiltrate the muscularis layer peripherally to the epithelial cells or enter the luminal space (arrows); HE, scale bar = 50 μ m. **C.** Collecting tubule with an abundant luminal accumulation of melanogenic macrophages; HE, scale bar = 50 μ m. **D.** Melanogenic macrophages and epithelial cells of a collecting duct; the cell's basophilic luminal border indicates a degenerative process (arrow); HE, scale bar = 10 μ m. **E.** Area of focal necrosis involving the collecting duct epithelium with melanogenic macrophage infiltrate (arrowhead); hyaline deposits in the cytoplasm of tubular epithelial cells (asterisk) are observed; HE, scale bar = 50 μ m.

Structural volumetric density. Lymphohematopoietic tissue was the most prevalent, followed by the proximal and distal tubules and blood vessels (Tab. 2). The sex effect was observed only in the lymphohematopoietic tissue. The correlation coefficients between renal structure and renosomatic index were positive for lymphohematopoietic tissue and proximal tubules and negative for distal tubules, blood vessels, collecting ducts, and melano-macrophage aggregates.

Histometric analysis of the renal corpuscle. Renal corpuscle, glomerular, and Bowman's space area were higher in the females. Parietal layer thickness was not significant and ranged from 0.35 to 0.47 μm . The significant variables are represented in the Fig. 5.

Macrophages melanogenic histochemistry. There was no sex effect on hemosiderin and lipofuscin content in the melano-macrophage aggregates and RSI correlation. Both pigments were well-differentiated (Fig. 6). Hemosiderin was found at a higher frequency than lipofuscin.

TABLE 2 | Mean standard error (\pm) and confidence interval (IC 95%) of volumetric density estimative (%) by sex, P value (P) showing no differences between males and females, and Pearson's correlation coefficient (r) with renosomatic index in the caudal kidney in *Pygocentrus nattereri* showing significant correlation with body weight and standard length (*). ns = non-significant values. \pm = standard error of the mean, N = specimens number, * $p < 0.05$, ** $P < 0.01$, MMA = melano-macrophages aggregates.

Parameters	Male (N = 15)	Female (N = 14)	P	r
Hematopoietic tissue	47.3 \pm 1.2 (44.4–51.4)	51.6 \pm 1.5 (45.5–56.3)	0.032	0.45**
Proximal tubule	18.4 \pm 0.6 (16.5–20.3)	18.0 \pm 0.8 (15.9–20.5)	0.71	0.37*
Distal tubule	15.6 \pm 0.7 (13.4–17.3)	14.1 \pm 0.9 (10.4–17.3)	0.19	-0.56**
Blood vessels	10.5 \pm 0.9 (7.5–13.5)	8.8 \pm 1.1 (7.7–9.9)	0.209	-0.34*
Collecting tubule	2.3 \pm 0.2 (1.4–3.1)	2.5 \pm 0.3 (2.1–3.1)	0.484	ns
Renal corpuscle	1.5 \pm 0.1 (1.4–1.6)	1.2 \pm 0.1 (1.0–1.3)	0.127	ns
Collecting duct	1.3 \pm 0.3 (0.2–1.5)	1.0 \pm 0.3 (0.2–1.7)	0.571	-0.47**
MMA	0.3 \pm 0.05 (0.16–0.47)	0.2 \pm 0.06 (0.04–0.31)	0.065	-0.34*

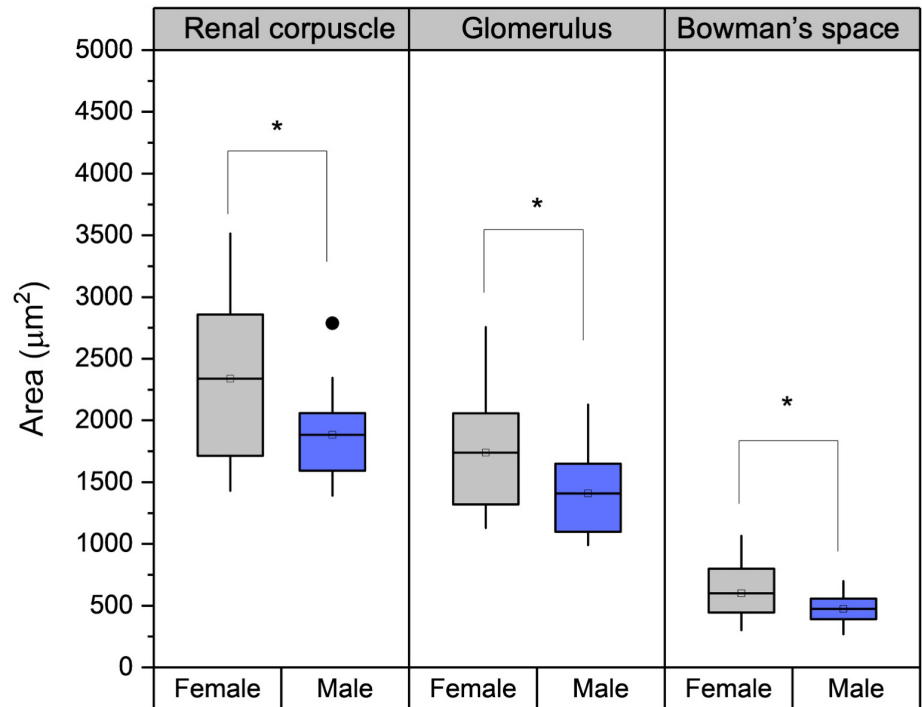


FIGURE 5 | Box plot (median, 25 and 75th quartile) and lines inside represent the median for the area of the Bowman's space, renal capsule and glomerulus of female and male of *Pygocentrus nattereri*. The points represent outliers and (*) show differences between female and male = $p < 0.05$.

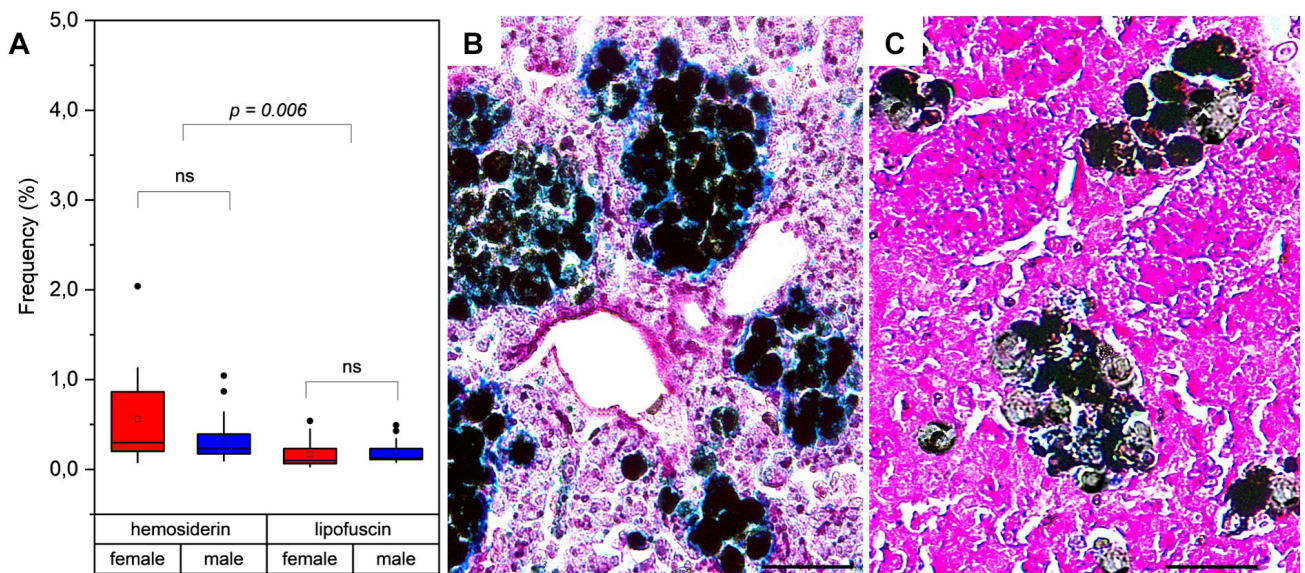


FIGURE 6 | Frequency of hemosiderin and lipofuscin in the caudal kidney melanomacrophages centers (MMC) of *Pygocentrus nattereri*. **A.** Frequency of area of pigments in tissue of female and male (mean, bars = epm). Differences between substances was observed (*), $P = 0.006$. **B.** Histological section stained with Perl's method for ferric iron for hemosiderin detection (arrow). **C.** Histological sections stained with Schmorl's solution for lipofuscin detection (arrow); scale bars = 50 µm.

DISCUSSION

Although the anatomical and histological descriptions of the kidneys in several freshwater fish species are well known, few studies have reported the histometric aspects as well as the importance of these techniques for morphofunctional studies. *Pygocentrus nattereri* has been recognized as a potential bioindicator of aquatic environments by detailed ecological, reproductive, parasitological, and phylogeographic studies (Uetanabaro *et al.*, 1993; Hubert *et al.*, 2007; Vicentin *et al.*, 2013; Ferreira *et al.*, 2014); however, the morphological basis of many essential organs remains poorly understood.

The general anatomical and histological features of the caudal kidney in *P. nattereri* are similar to those of other Characiformes freshwater fish with some particularities (Dantzler *et al.*, 2016). The cephalic kidney was detached from the caudal kidney through a robust vascular network, which is a distinct characteristic of this species. Thus, in this study, the kidney weight used to calculate the renosomatic index referred to the caudal portion of the kidney. Furthermore, the renosomatic index was negatively correlated with body weight and standard length, possibly because of allometric growth, which is typically pronounced after sexual maturity (Siqueira *et al.*, 2021). Most of the populations studied consisted of sexually mature specimens, but not all had reached their maximum growth. As there was no sex effect on kidney weight, the negative coefficients suggest that this organ develops rapidly in young individuals, decreasing its relationship while gaining weight and length.

In the structural volumetric density analysis, it was verified that the lymphohematopoietic tissue and proximal tubules had the highest density. Lymphohematopoietic tissue is responsible for the proliferation and storage of different leukocyte cell lineages and in the exocrine kidney. Granulocytic and agranulocytic leukocytes constitute the largest population of cells in this segment although some rodlet cell niches were also observed. Thus, our findings suggest that rodlet cells may play a sentinel role in this renal compartment (Desfuli *et al.*, 2022). The basic structure and cell distribution of lymphohematopoietic tissue is very similar to those of other fish bodies. Despite not finding a network of sinusoidal reticuloepithelium, the type and cell arrangement suggest a comparative function as an extension of the cephalic kidney (Takashima, Hibiya, 1995; Mokhtar, 2017). In this study, females had a higher percentage of lymphohematopoietic tissue than males, probably due to a hormonal effect previously reported in *Salmo trutta* (Resende *et al.*, 2010). Nevertheless, this tissue increased in proportion to the renosomatic index in both males and females. Thus, variations in this relationship may be helpful in the study of pathological conditions affecting the immune system (Camargo, Martinez, 2007; Xu *et al.*, 2016; Ciulli *et al.*, 2020).

There are relatively few differences in the tubular vasculature of caudal kidneys in fish. Consequently, blood flow from the renal artery enters the glomerulus, the vascularized portion of the renal corpuscle, to initiate the plasma clearance process (Hentschel *et al.*, 2000). The glomerular filtrate flows toward the proximal and distal tubules, tubules, and collecting ducts to the ureter. Among these, the proximal and distal tubules account for approximately one-third of the organ volume, both of which correlate with the renosomatic index. The inverse correlation observed between tubule segments and RSI may be due to the functional particularities of the epithelial cells. Proximal

tubules presenting epithelial cells rich in brush borders (microvilli) amplify the cell surface area in contact with luminal ultrafiltrate, more than half of which is reabsorbed in the proximal tubule (Peery, 2011; Dantzler, 2016). Thus, amino acids, inorganic phosphate, and some solutes are resorbed via secondary active transport, which may remain stored in the cytoplasm in the form of hyaline granules, as commonly noted in several samples (Takashima, Hibiya, 1995; Fernandes *et al.*, 2019). In contrast, the distal tubules and collecting ducts are involved in the passive reabsorption of sodium and chlorides for osmotic and blood pressure equilibrium (Raidal, Raidal, 2006; Dantzler, 2016). Therefore, the negative association between the renosomatic index and the distal tubule, collecting duct, and blood vessels might be due to the intrinsic regulation of the final caudal function from kidney maturation.

Histometric measurements of the renal corpuscles were higher in female specimens. The glomerular filtration rate of a single nephron is determined by pressure gradients, hydraulic conductivity, and the surface area over which filtration occurs (McMillan, 2011). Thus, although the relative volumetric density of the renal corpuscles has been similar between the sexes, the histometric differences suggest that female *P. nattereri* may tend to have a higher glomerular filtration rate. On the other hand, such differences may represent subtle adaptations from the endocrine, seasonal and osmoregulatory mechanisms (Handerson *et al.*, 1985; Resende *et al.*, 2010; Dantzler, 2016).

The MMs density was less than one percent of the renal structures set evaluated, negatively correlated with RSI, suggesting that these structures tend to reduce as individuals become adults. These values are well below those previously reported for *Salvelinus fontinalis* (Mitchill, 1814), *Oncorhynchus mykiss* (Walbaum, 1792), and *Gymnotus inaequilabiatus* (Valenciennes, 1839) (Schwindt *et al.*, 2006; Fernandes *et al.*, 2019). The frequency of hemosiderin of MMs was higher than that of lipofuscin, without sex effect. While hemosiderin remains an endogenous phagocytosis material of cells, lipofuscin is an undegradable material that has previously undergone autophagocytosis induced by elevated oxidative stress in response to innate immunity (Brunk, Termann, 2002; Agius, Roberts, 2003). In this sense, both pigments are involved in the innate defense processes into the hematopoietic tissue of the kidney.

This is the first comparative study in *P. nattereri* conducted for the caudal kidney morphological baseline between males and females. The renosomatic index is associated with various functional structures and its variation accounts for the volumetric density of lymphohematopoietic tissue and the proximal and distal tubular segments. The particularity of the sex effect may define punctual differences in future studies on the metabolism and immunity of this species. Lymphohematopoietic tissue has a higher volumetric structure but differs between males and females. Despite their low density in renal tissue, MMs seem to be abbreviated for other species. The importance of knowing the morphology of the caudal kidneys and possible morphological variation factors can direct future studies of environmental monitoring or experimental studies.

REFERENCES

- **Agius C, Roberts RJ.** Melano-macrophage centres and their role in fish pathology. *J Fish Dis.* 2003; 26(9):499–509. <https://doi.org/10.1046/j.1365-2761.2003.00485.x>
- **Alho C.** The Pantanal. In: Fraser LH, Keddy PA, editors. *The world's largest wetlands-ecology and conservation.* Cambridge: Cambridge University Press; 2005. p.203–71. Available from: <https://doi.org/10.1017/CBO9780511542091.008>
- **Brunk UT, Terman A.** Lipofuscin: mechanisms of age-related accumulation and influence on cell function. *Free Radical Bio Med.* 2002; 33(5):611–19. [https://doi.org/10.1016/S0891-5849\(02\)00959-0](https://doi.org/10.1016/S0891-5849(02)00959-0)
- **Burger J.** Bioindicators: Types, development, and use in ecological assessment and research bioindicators in ecological assessment and research. *Environ Bioindic.* 2006; 1:22–39. <https://doi.org/10.1080/15555270590966483>
- **Camargo MMP, Martinez CBR.** Histopathology of gills, kidney and liver of a Neotropical fish caged in an urban stream. *Neotrop Ichthyol.* 2007; 5(3):327–36. <https://doi.org/10.1590/S1679-62252007000300013>
- **Campbell JH, Dixon B, Whitehouse LM.** The intersection of stress, sex and immunity in fishes. *Immunogenetics.* 2021; 73:111–29. <https://doi.org/10.1007/s00251-020-01194-2>
- **Carson FL, Hladik C.** Brown-Hopps modification of the Gram stain. In: *Histotechnology: a self instructional text.* 2009. p.231–33.
- **Ciulli S, Volpe E, Sirri R, Tura G, Errani F, Zamperin G et al.** Multifactorial causes of chronic mortality in juvenile sturgeon (*Huso huso*). *Animals.* 2020; 10(10):1866. <https://doi.org/10.3390/ani10101866>
- **Dantzer WH.** Renal morphology. In: *Transport of fluid by renal tubules.* New York: The American Physiological Society, Springer; 2016. p.159–71.
- **Desfuli BS, Pironi F, Maynard B, Simoni E, Bosi G.** Rodlet cells, fish immune cells and a sentinel of parasitic harm in teleost organs. *Fish Shellfish Immunol.* 2022; 121:516–34. <https://doi.org/10.1016/j.fsi.2021.09.045>
- **Fernandes CE, Marcondes SF, Galindo GM, Franco-Belussi L.** Kidney anatomy, histology and histometric traits associated to renosomatic index in *Gymnotus inaequilabiatus* (Gymnotiformes: Gymnotidae). *Neotrop Ichthyol.* 2019; 17(4):e190107. <https://doi.org/10.1590/1982-0224-20190107>
- **Ferreira CMA, Egler SG, Vallouz AV, Ignácio ARA.** Semiquantitative determination of total mercury in *Pygocentrus nattereri* Kner, 1858 and sediment at the plateau of upper Paraguai River, Brazil. *Chemosphere.* 2017; 174:604–12.
- **Ferreira T, Rasband W.** ImageJ User Guide: IJ 1.46r; 2014. Available from: <http://imagej.nih.gov/ij/docs/guide>
- **Ferreira FS, Vicentin W, Costa FEDS, Suárez YR.** Trophic ecology of two piranha species, *Pygocentrus nattereri* and *Serrasalmus marginatus* (Characiformes, Characidae), in the floodplain of the Negro River, Pantanal. *Acta Limnol Bras.* 2014; 26:381–91. <https://doi.org/10.1590/S2179-975X2014000400006>
- **Franco-Belussi L, Castrucci AML, Oliveira C.** Responses of melanocytes and melanomacrophages of *Eupemphix nattereri* (Anura: Leiuperidae) to Nle4, D-Phe7- α melanocyte stimulating hormone and lipopolysaccharides. *Zoology.* 2013; <https://doi.org/809.10.1016/j.zool.2013.06.003>
- **Froese R, Pauly D.** FishBase [Internet]. World Wide Web electronic publication. 2020. Available from: <http://www.fishbase.org>
- **Handerson IW, Hazon NEIL, Hughes K.** Hormones, ionic regulation and kidney function in fishes. In: *Symposia of the Society for Experimental Biology.* 1985; 39:245–65.
- **Hentschel H, Elger M, Dawson M, Rendro MD.** Urinary Tract. In: Ostrander GK, editor. *The laboratory fish.* Academic Press; 2000. p.181–87.
- **Hubert N, Duponchelle F, Nunez J, Garcia-Davila C, Paugy D, Renno J-F.** Phylogeography of the piranha genera *Serrasalmus* and *Pygocentrus*: implications for the diversification of the Neotropical ichthyofauna. *Mol Ecol.* 2007;16(10):2115–36. <https://doi.org/10.1111/j.1365-294X.2007.03267.x>

- **Idrus SNS, Abdullah MR, Mohd FH, Othman MS.** Hepatosomatic and renosomatic indices of *Anabas testudineus* exposed to various levels of cadmium. *J Environ Prot.* 2000; 13(1):161–70. <https://doi.org/10.4236/jep.2022.131010>
- **McDonald MD, Smith CP, Walsh PJ.** The physiology and evolution of urea transport in fishes. *J Membr Biol.* 2006; 212(2):93–107. <https://doi.org/10.1007/s00232-006-0869-5>
- **McMillan DB.** Histology of the Kidney. In: Farrel AP, editor. *Encyclopedia of fish physiology: from genome to environment.* Vol. 2. The Gut. Role of the Kidneys. Elsevier; 2011. p.1395–410.
- **Mokhtar DM.** Fish histology: from cells to organs. New York: Apple Academic Press; 2017. <https://doi.org/10.1201/9781315205779>
- **Nimet J, Amorim JPA, Delariva RL.** Histopathological alterations in *Astyanax bifasciatus* (Teleostei: Characidae) correlated with land uses of surroundings of streams. *Neotrop Ichthyol.* 2018;16(1):e170129. <https://doi.org/10.1590/1982-0224-20170129>
- **Novakowski GC, Hahn NS, Fugi R.** Diet seasonality and food overlap of the fish assemblage in a pantanal pond. *Neotrop Ichthyol.* 2008; 6(4):567–76. <https://doi.org/10.1590/S1679-62252008000400004>
- **Nyengaard JR.** Stereologic methods and their application in kidney research. *J Am Soc Nephrol.* 1999; 10(5):1100–23. <https://doi.org/10.1681/ASN.V1051100>
- **Pauly D.** Quantitative analysis of published data on the growth, metabolism, food consumption, and related features of the red-bellied piranha, *Serrasalmus nattereri* (Characidae). *Environ Biol Fish.* 1994; 41:423–37. <https://doi.org/10.1007/BF02197858>
- **Perry SF.** The Kidney. In: Farrel AP, Jr, Cech JJ, Richards JG, Stevens ED, editors. *Encyclopedia of fish physiology. From genome to environment.* Vol 2. Academic Press, Elsevier; 2011. p.1411–18.
- **Raidal SR, Raidal SL.** Comparative renal physiology of exotic species. *Vet Clin North Exot Anim Practi.* 2006; 9(1):13–31.
- **Rašković B, Cruzeiro C, Poleksić V, Rocha E.** Estimating volumes from common carp hepatocytes using design-based stereology and examining correlations with profile areas: Revisiting a nutritional assay and unveiling guidelines to microscopists. *Microsc Res Techn.* 2019; 82(6):861–71. <https://doi.org/10.1002/jemt.23228>
- **Reid IM.** Morphometric methods in veterinary pathology: A review. *Vet Pathol.* 1980; 17(5):522–43. <https://doi.org/10.1177/030098588001700502>
- **Resende AD, Lobo-da-Cunha A, Malhão F, Franquinho F, Monteiro RAF, Rocha E.** Histological and stereological characterization of brown trout (*Salmo trutta* f. fario) trunk kidney. *Microsc Microanal.* 2010; 16(6):677–87. <https://doi.org/10.1017/S1431927610093918>
- **Roberts RJ, Ellis AE.** The anatomy and physiology of Teleosts. In: Roberts RJ, editor. *Fish pathology.* 2012. p.17–61. <https://doi.org/10.1002/9781118222942.ch2>
- **Rocha E, Monteiro RAF, Pereira CA.** Liver of the brown trout, *Salmo trutta* (Teleostei, Salmonidae): A stereological study at light and electron microscopic levels. *Anat Rec.* 1997; 247(3):317–28. [https://doi.org/10.1002/\(SICI\)1097-0185\(199703\)247:3<317::AID-AR3>3.0.CO;2-R](https://doi.org/10.1002/(SICI)1097-0185(199703)247:3<317::AID-AR3>3.0.CO;2-R)
- **Schwindt AR, Truelove N, Schreck CB, Fournie JW, Landers DH, Kent ML.** Quantitative evaluation of macrophage aggregates in brook trout *Salvelinus fontinalis* and rainbow trout *Oncorhynchus mykiss*. *Dis Aquat Organ.* 2006; 68(2):101–13. <https://doi.org/doi:10.3354/dao068101>
- **Siqueira MS, Leão TRF, Rodrigues RA, Farias KNN, Silva ALN, Marcondes SF et al.** Age-associated hemogram and ultrastructural leukocyte morphology in *Pygocentrus nattereri* (Characiformes: Serrasalminidae) from the Brazilian Pantanal. *Neotrop Ichthyol.* 2021; 19(1):e200136. <https://doi.org/10.1590/1982-0224-2020-0136>
- **Takashima F, Hibiya T.** An atlas of fish histology: normal and pathological features. 2nd ed, Tokyo: Kondansha; 1995.
- **Uetanabaro M, Wang T, Abe AS.** Breeding behaviour of the red-bellied piranha, *Pygocentrus nattereri*, in nature. *Environ Biol Fishes.* 1993; 38:369–71. <https://doi.org/10.1007/BF00007529>

- **Vicentin W, Vieira KRI, Tavares LER, Costa FES, Takemoto RM, Paiva F.** Metazoan endoparasites of *Pygocentrus nattereri* (Characiformes: Serrasalminae) in the Negro River, Pantanal, Brazil. *Rev Bras Parasitol Vet.* 2013; 22(3):331–38. <https://doi.org/10.1590/S1984-29612013000300003>
- **Vize PD.** A Homeric view of kidney evolution: A reprint of HW Smith's classic essay with a new introduction. *Anat Rec.* 2004; 277(2):344–54. <https://doi.org/10.1002/ar.a.20017>
- **Xu H-J, Jiang W-D, Feng L, Liu Y, Wu P, Jiang J et al.** Dietary vitamin C deficiency depresses the growth, head kidney and spleen immunity and structural integrity by regulating NF-κB, TOR, Nrf2, apoptosis and MLCK signaling in young grass carp (*Ctenopharyngodon idella*). *Fish Shellfish Immunol.* 2016; 52:111–38. <https://doi.org/10.1016/j.fsi.2016.02.033>

AUTHORS' CONTRIBUTION

Sandriely F. Marcondes: Formal analysis, Methodology.

Mayara S. Siqueira: Conceptualization, Methodology.

Taynara R. F. Leão: Conceptualization, Methodology.

Robson A. Rodrigues: Conceptualization, Formal analysis, Methodology.

Karine N. N. Farias: Formal analysis, Methodology.

André L. N. Silva: Investigation, Methodology.

Lilian Franco-Belussi: Formal analysis, Methodology, Writing-review and editing.

Carlos E. Fernandes: Conceptualization, Formal analysis, Funding acquisition, Investigation, Writing-original draft, Writing-review and editing.

ETHICAL STATEMENT

Animal handling are in accordance with the Ethics Committee on Animal Use (CEUA/UFMS, protocol 801/2016) and the Sistema de Autorização e Informação em Biodiversidade (SISBIO, project no. 51270–1) approved the procedures used in this study.

COMPETING INTERESTS

The author declares no competing interests.

HOW TO CITE THIS ARTICLE

- **Marcondes SF, Siqueira MS, Leão TRF, Rodrigues RA, Farias KNN, Silva ALN, Franco-Belussi L, Fernandes CE.** Morphological and histometric features of the caudal kidney in piranha *Pygocentrus nattereri* (Characiformes: Serrasalminidae). *Neotrop Ichthyol.* 2023; 21(2):e220108. <https://doi.org/10.1590/1982-0224-2022-0108>

Neotropical Ichthyology

OPEN ACCESS



This is an open access article under the terms of the Creative Commons Attribution License, which permits use, distribution and reproduction in any medium, provided the original work is properly cited.

Distributed under Creative Commons CC-BY 4.0

© 2023 The Authors. Diversity and Distributions Published by SBI



Official Journal of the Sociedade Brasileira de Ictiologia